Two dimensional singularity turbulence

Juliette Amauger, Christophe Josserand, Yves Pomeau, Sergio Rica

Two dimensional singularity turbulence

Juliette Amauger[1], Christophe Josserand[1], Yves Pomeau[1] and Sergio Rica[2]

[1] *LadHyX, CNRS & Ecole Polytechnique, UMR 7646, IP Paris, 91128, Palaiseau, France.*
[2] *Instituto de Física, Facultad de Física, Pontificia Universidad Católica de Chile, Casilla 306, Santiago, Chile.*

Abstract

Using the self-focusing non-linear Schrödinger (NLS) equation, we suggest a singularity-mediated turbulent scenario. This equation is taken as a simple (toy) model to investigate the role of potential singularities in fully developed turbulence and intermittencies. The self-focusing NLS equation has the advantage to exhibit finite-time singular solutions in any dimension D, which are described by a simple solution of a nonlinear self-similar universal equation. We investigate in this paper in particular the two dimensional (2D) dynamics which provides a more complex behavior than the 1D case studied formerly. The current scenario of turbulence offers an understanding of the role of singularities in dissipation in a turbulent flows and reproduces, among other aspects, the observed anomaly of dissipation in the limit of zero viscosity.

Keywords: Non-linear Schrödinger equation, finite-time singularities, Turbulent dissipation, Inttermitency, Anomalous dissipation

1. Introduction

Singularities and turbulence have always been in a dangerous relationship. At first, it concerns the incompressible Navier-Stokes equation that describes the dynamics of incompressible simple fluids, as water, and provides the good framework to study turbulence. Already, the question whether this Navier-Stokes equation exhibits or not finite-time singularities (for smooth initial conditions) remains an open problem despite the tremendous efforts of the scientific community, tracing back to the pioneering work of Leray for the case of the Navier-Stokes equations [1]. The analogous question of the existence of finite-time singularities for the inviscid case ruled by the Euler equations also remains an open problem (see for instance [2, 3, 4, 5]). Furthermore, the classical theories of turbulence, following the work of Kolmogorov [6] provides a power spectrum for the velocity fluctuations that is a wonderful example of a singular limit. Indeed, the von Kármán-Howarth-Monin relationship [7] relates the statistical mean value of the velocity increment $\delta\boldsymbol{v} = \boldsymbol{v}(\boldsymbol{x}_0+\boldsymbol{x}) - \boldsymbol{v}(\boldsymbol{x}_0)$, between two points separated by a distance $x = |\boldsymbol{x}|$ to the energy dissipation rate per unit mass, ϵ (with dimensions of L^2/T^3), through the scaling $\delta v \sim (\epsilon x)^{1/3}$.

This relationship is valid in the inertial regime where viscosity can be neglected, that means for length larger than the Kolmogorov length $\lambda_K \sim (\nu^3/\epsilon)^{1/4}$, where ν is the kinematic viscosity of the fluid. The singular limit arises thus naturally when considering vanishing ν, leading to a finite dissipation rate ϵ (the so-called zero-th law of turbulence) while the spatial derivative of the mean value of the velocity increment is no longer defined. Finally, signature of turbulent behaviors are often invoked to justify the intermittency properties of the turbulent fields [8]. Therefore, since the existence (and the form) of finite-time singularities in the Navier-Stokes equations remains undetermined, the influence of such possible singular flows (even if they would be eventually regularized at short scales) to the statistical properties of turbulent flows cannot be evaluated.

Recently, three of us have considered a much simpler model where the existence of finite-time singularities in the limit equation without dissipation is well known and characterized, allowing to study how a turbulent dynamics in such system is affected by the occurrence of these very intense events as viscosity is switched on [9]. We have shown, that, despite its simplicity, our model in one spatial dimension exhibits both, intermittency (the dynamics appears as a random sequence of peaks, corresponding to viscosity-regularized potential singularities), and, a turbulent cascade spectrum, although in these systems no cascade processes towards small scales can be identified.

The model is in fact deduced from the focusing nonlinear Schrödinger (NLS later on) equation to which forcing at large scale and dissipation at small scales are added, which reads:

$$i\frac{\partial \psi}{\partial t} = -\frac{\alpha}{2}\boldsymbol{\nabla}^2\psi - g|\psi|^{2n}\psi - i\nu\Delta^2\psi + f(\boldsymbol{x},t), \qquad (1)$$

where $\psi(\boldsymbol{x},t)$ is a complex field representing a wave amplitude which can be considered in general in a space of dimension D. The α term represents the wave dispersion, and g the strength of the nonlinear dependence of oscillation frequency, $g|\psi|^{2n}$, on the wave amplitude $|\psi|$. The term $-i\nu\Delta^2\psi$ in (1) denotes a damping which we have chosen to be of higher order in derivatives than the inviscid and conservative case ($\nu = 0$). Finally, $f(\boldsymbol{x},t)$ is an additive complex forcing that acts at large scales. Equation (1) is complemented with a smooth initial condition. In the present paper, we study this model in two space dimensions (2D) and investigate how the existence of singularities in the inviscid limit influences the turbulent dynamics when dissipation and forcing are present.

The paper is organized as follows: next section 2 introduces the inviscid nonlinear Schrödinger equation which is the basic model under study. Section 3 summarizes the main characteristic of the well known singular finite-time blow-up in the inviscid nonlinear Schrödinger equation. Before the conclusion, section 4 describe the observed features of a singularity-mediated turbulence in this 2D NLS equation (1).

2. The focusing nonlinear Schrödinger Model

In what follows we firstly consider the focusing nonlinear Schrödinger (NLS) equation with zero damping and zero forcing, that is,

$$i\frac{\partial\psi}{\partial t} = -\frac{\alpha}{2}\boldsymbol{\nabla}^2\psi - g|\psi|^{2n}\psi. \quad (2)$$

Here, $\psi(\boldsymbol{x},t)$ is a complex field defined in an infinite space of dimension D.

Since the hyper-viscosity ν and the forcing vanish here, one recovers the usual $(2n+1)$-th order nonlinear Schrödinger equation which is explicitly conservative and reversible. Indeed, from the NLS equation one derives the following conservation laws.

2.1. Mass conservation

The "density" $|\psi|^2 \equiv \psi\bar{\psi}$, where $\bar{\psi}$ means the complex conjugated field of ψ, follows a conservative dynamics

$$\partial_t|\psi|^2 + \partial_i j_i = 0, \quad (3)$$

where the current is defined by

$$j_i = -\frac{i\alpha}{2}\left(\bar{\psi}\partial_i\psi - \psi\partial_i\bar{\psi}\right). \quad (4)$$

In equation (3), as well as, in equations (6) and (9) below, the indices run $\{i,k\} = 1,2,\ldots D$ and repeated indices stand for a sum following Einstein's convention.

The conservation law (3) implies that the total mass (or number of particles in the context of Bose-Einstein condensates, light intensity in nonlinear optics)

$$N = \int |\psi|^2 d^D\boldsymbol{x} \quad (5)$$

remains constant in time.

2.2. Momentum conservation

The current, which is a momentum density flow, rules

$$\partial_t j_i + \partial_k T_{ik} = 0, \quad (6)$$

where T_{ik} is a stress tensor:

$$T_{ik} = \frac{\alpha^2}{4}\left(\partial_i\bar{\psi}\partial_k\psi + \partial_i\psi\partial_k\bar{\psi} - \bar{\psi}\partial_{ik}\psi - \psi\partial_{ik}\bar{\psi}\right) - \frac{\alpha g n}{n+1}|\psi|^{2(n+1)}\delta_{ik}. \quad (7)$$

Interestingly, the term $p = -\frac{\alpha g n}{n+1}|\psi|^{2(n+1)}$ represents an isotropic pressure which has a negative sign for $\alpha g > 0$, whence an uniform solution becomes linearly unstable since $\frac{\partial p}{\partial|\psi|^2} \leq 0$. Therefore, in the long wave limit this system

develops a linear instability. However, we underline that the short wavelength perturbations are dispersive modes, hence the short wavelength modes do not grow exponentially in time. Any initial perturbation of the uniform solution grows thus exponentially at short time with a well defined bandwidth wavelength.

Finally, the force per unit area acting on a boundary is given by the components of the stress tensor (7): $f_i = T_{ik}\hat{n}_k$, where $\hat{n}_k$ is the unitary normal vector to the desired surface.

2.3. Energy conservation

Contrary to fluid dynamics, the energy of the focusing NLS equation, involves two terms of opposite signs, allowing the possibility that the relevant energy is not a positive defined quantity. Indeed, the energy density reads,

$$\mathcal{E} = \left(\frac{\alpha}{2} |\boldsymbol{\nabla}\psi|^2 - \frac{g}{n+1} |\psi|^{2(n+1)} \right), \tag{8}$$

and, it obeys a conservation equation

$$\partial_t \mathcal{E} + \partial_k Q_k \quad = \quad 0, \tag{9}$$

where the energy flux is given by

$$Q_k = \frac{i}{2} \left[\left(\frac{\alpha}{2} \nabla^2 \bar{\psi} - g|\psi|^{2n} \bar{\psi} \right) \partial_k \psi - cc. \right].$$

Here *c.c.* stands for complex conjugated. Therefore, the total energy or Hamiltonian,

$$H = \int \left(\frac{\alpha}{2} |\boldsymbol{\nabla}\psi|^2 - \frac{g}{n+1} |\psi|^{2(n+1)} \right) d^D \boldsymbol{x}, \tag{10}$$

is conserved by the dynamics of (2).

3. Blow-up solutions of the nonlinear Shchrödinger equation.

In what follows we show that under some conditions the perturbation amplitude blows-up in finite-time in the inviscid case ($\nu = 0$) and for the sake of simplicity we set $\alpha = g = 1$ without loss of generality.

3.1. Self-similar Wave collapse for the inviscid limit.

One of the features of the un-forced and inviscid limit (2) is that it displays, in the cases where $nD > 2$, a finite-time singularity at a given point (a position and a time that depends explicitly on the shape of the initial condition). This makes the great difference with respect to the inviscid fluid case, namely the Euler equations, where the existence of such a singular solutions are in fact still an open question on the way of being solved positively (hopefully).

The existence of this finite-time singularity is due to the non positiveness of the energy density, which is the difference of two positive terms that can both become large (and infinite at the singularity) while their difference remains constant. In fact, defining $\left\langle |\boldsymbol{x}|^2 \right\rangle = \int |\boldsymbol{x}|^2 |\psi(\boldsymbol{x},t)|^2 d^D\boldsymbol{x}$, the arguments for the finite-time singularity, following Talanov [10] and Zakharov [11], come from the dynamical relation :

$$\frac{d^2}{dt^2}\left\langle |\boldsymbol{x}|^2 \right\rangle \;=\; 4\alpha H - \frac{2(nD-2)}{(n+1)}\int |\psi(\boldsymbol{x},t)|^{2(n+1)} d^D\boldsymbol{x}, \tag{11}$$

therefore if $nD > 2$ one has $\frac{d^2}{dt^2}\left\langle |\boldsymbol{x}|^2 \right\rangle \leq 8H$. Moreover because H is constant, $\left\langle |\boldsymbol{x}|^2 \right\rangle \leq 2\alpha H t^2 + c_1 t + c_0$, thus, if initially $H \leq 0$ necessarily it exists a t_c, such that $\left\langle |\boldsymbol{x}|^2 \right\rangle \to 0$ as $t \to t_c$. Then, applying the Cauchy-Schwarz inequality:

$$\int |\psi|^2 d^D\boldsymbol{x} \leq \left(\int |\nabla\psi|^2 d^D\boldsymbol{x}\right)\left(\int x_i x_i |\nabla\psi|^2 d^D\boldsymbol{x}\right)$$

implies that at the singularity $\int |\boldsymbol{\nabla}\psi|^2 d^D\boldsymbol{x} \to \infty$, indicating the presence of a finite time singularity. In fact, there is abundant evidence of the existence of self-similar finite-time blow-up solutions with an amplitude that increases in a contracting region that vanishes at the collapsing time [12, 13]. Seeking a radial symmetric solution ($r = |\boldsymbol{x}|$)

$$\psi(r,t) \;=\; \frac{1}{(t_c-t)^{1/2n}}\Phi\left(\frac{r}{(t_c-t)^{1/2}}, -\log(t_c-t)\right), \tag{12}$$

then the self-similar function $\Phi(\xi,\tau)$ that depends on the self-similar variables $\xi = r/(t_c-t)^{1/2}$ and $\tau = -\log(t_c-t)$ rules the following partial differential equation

$$i\frac{\partial}{\partial\tau}\phi(\xi,\tau) + \frac{i}{2}\left(\frac{1}{n} + \xi\frac{\partial}{\partial\xi}\right)\phi = -\frac{1}{2}\left(\frac{\partial^2\phi}{\partial\xi^2} + \frac{D-1}{\xi}\frac{\partial\phi}{\partial\xi}\right) - |\phi|^{2n}\phi. \tag{13}$$

This equation admits "oscillatory" solutions in τ of the form: $\phi(\xi,\tau) = e^{i\lambda\tau}\varphi(\xi)$, where $\varphi(\xi)$ satisfies the ordinary differential equation:

$$-\lambda\varphi(\xi) + \frac{i}{2}\left(\frac{1}{n}\varphi + \xi\varphi'\right) = -\frac{1}{2}\left(\varphi'' + \frac{D-1}{\xi}\varphi'\right) - |\varphi|^{2n}\varphi, \tag{14}$$

which is complemented by the boundary conditions:

$$\varphi(0) = \varphi_0,\ \varphi'(0) = 0,\ \&\ \varphi(\xi) \sim \xi^{-1/n},\ \xi \to \infty. \tag{15}$$

Because of phase invariance of (14) it is possible to set φ_0 real. The real parameters λ and φ_0 make possible the integration of (14), however for an arbitrary pair of numbers (λ, φ_0), the solution of the ode (14) displays an oscillatory behavior in the limit $\xi \to \infty$, whence the solution does not satisfy the right boundary

conditions (15). The selection mechanism follows by simple counting the free available parameters (λ, φ_0) and the number of conditions required to satisfy a non-oscillatory behavior when $\xi \to \infty$ (this is simply the linear part of (15)). In the present case, the asymptotic condition selects the right values for (λ, φ_0).

It has been shown that there are infinite solutions that satisfy the equation (14) together with the boundary condition (15). We label with an index $\ell = 0, 1, 2, \ldots$, the solutions φ_ℓ, which are characterized by the "nonlinear eigenvalue" λ_ℓ and the finite amplitude $\varphi_0^{(\ell)}$.

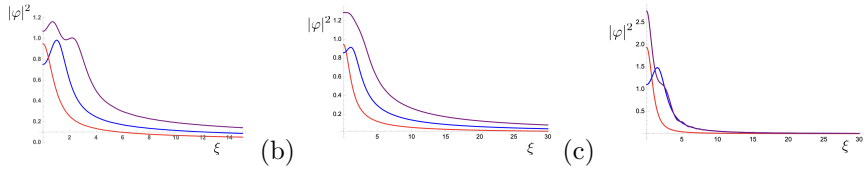

Figure 1: Plot of the numerical solution self-similar ordinary differential equation (14) with the boundary conditions (15) for different dimensions. The plots show three distinct numerical solutions for three different couple of parameters (φ_0, λ). In particular, at each plot, the red solution represents the zero energy solution (see below). (a) The one dimensional case for $n = 3$. (b) The two dimensional case $D = 2$ with $n = 2$. (c) The three dimensional case $D = 3$ with $n = 1$.

The figure 1 shows numerical simulations of the self-similar ordinary differential equation (14) with the boundary conditions (15) that do not present any oscillatory asymptotic behavior. The following table summarizes the firstvalues of the parameter λ_ℓ and $\varphi_0^{(\ell)}$.

case	$\ell = 0$	$\ell = 1$	$\ell = 2$
$d = 1 \,\&\, n = 3$	$\lambda = 0.3598 \quad \varphi_0 = 0.975$	$\lambda = 0.707 \quad \varphi_0 = 0.8675$	$\lambda = 1.4175 \quad \varphi_0 = 1.035$
$d = 2 \,\&\, n = 2$	$\lambda = 0.32625 \quad \varphi_0 = 0.9795$	$\lambda = 0.861 \quad \varphi_0 = 0.926$	$\lambda = 1.134 \quad \varphi_0 = 1.662$
$d = 3 \,\&\, n = 1$	$\lambda = 0.545 \quad \varphi_0 = 1.3925$	$\lambda = 1.56 \quad \varphi_0 = 1.05$	$\lambda = 2.20 \quad \varphi_0 = 1.66$

Table 1: Summary of some the self-similar ordinary differential equation (14) with the boundary conditions (15) for $d = 1, 2, 3$ and various n. The column $\ell = 0$ correspond to the zero-energy, $\mathcal{H}_0$ solution (see main text).

The question is which one of these solutions is the selected one by the dynamics of NLS? We need to explore in more detail the conserved quantities. Near the wave collapse the "mass" of the singular solution defined through (5) becomes

$$N_{\text{collapse}} = \int |\psi|^2 d^D \boldsymbol{x} = (t_c - t)^{D/2 - 1/n} S_D \int_0^\infty |\varphi|^2 \, \xi^{D-1} \, d\xi$$

where S_D is the surface of a unit sphere in dimension D. Because $nD > 2$, then, $N_{\text{collapse}} \to 0$ as $t \to t_c$, therefore the mass of the singularity becomes zero at t_c. Notice that this is not the current total mass, because the self-similar solution of the nonlinear eigenvalue problem (14) suffers a mechanism of attraction of

an arbitrary initial condition to (12). The important aspect is that this process is not forbidden by a conservation law. Indeed, if the mechanism of attraction would require an infinite mass, the self-similar singularity would not be possible.

On the other hand, a similar analysis says that the Hamiltonian scales as $H = (t_c - t)^{D/2-1/n-1}\mathcal{H}_0$, hence it may diverge for $2 < nD < 2(n+1)$, in this case it is necessary to impose :

$$\mathcal{H}_0 = \int_0^\infty \left(\frac{1}{2} |\varphi'|^2 - \frac{1}{n+1} |\varphi|^{2(n+1)} \right) \xi^{D-1} d\xi \equiv 0. \tag{16}$$

It follows that the solution selected by the dynamics satisfy equation (14) together with the boundary condition (15) and the restriction (16). This solution is called the ground state ($\ell = 0$) and appears to be stable. It is thus the one observed in the time dependent numerical simulations of (2).

In summary, if $2 < nD < 2(n+1)$ and for a suitable smooth initial condition (in such a way that the initial Hamiltonian is negative), then the solution of (2) blows-up at a point (the solution and its gradient become infinite) in finite-time in a self-similar way such that the amplitude increases while the size of blow-up region decreases.

3.2. Pressure fluctuation as a consequence of a finite-time singularity.

We briefly discuss here the effect of a singularity on the momentum (7). This effect is given by the stress tensor, near the position where the singular blow-up has happened. The stress tensor (7) in 1D, possesses only a single component which is T_{xx}. Because of the symmetry of the singularity, we focus on the radial pressure in higher dimensiosn (in dimensions $D = 2$, & 3 here), which exhibits the same expression as the one in the one dimensional case:

$$T_{rr} \quad = \quad \hat{n}_i T_{ik} n_k = \frac{1}{4} \left(2|\partial_r \psi|^2 - \bar{\psi} \partial_{rr} \psi - \psi \partial_{rr} \bar{\psi} \right) - \frac{n}{n+1} |\psi|^{2(n+1)}.$$

After introducing the self-similar solution (12) into the previous radial stress expression, one obtains:

$$\begin{aligned} T_{rr} \quad &= \quad \frac{1}{(t_c - t)^{1+1/n}} \sigma(\xi) \quad \text{with} \\ \sigma(\xi) \quad &\equiv \quad \left(\frac{1}{4} \left(2|\varphi'|^2 - \bar{\varphi}\varphi'' - \varphi\bar{\varphi}'' \right) - \frac{n}{n+1} |\varphi|^{2(n+1)} \right), \end{aligned} \tag{17}$$

The stress field, T_{rr}, thus always diverges as $t \to t_c$, and its space evolution depends on the explicit self-similar solutions computed already. The far field behavior for the singular solution being

$$\psi \approx A \xi^{-\frac{1+2i\lambda n}{n}},$$

for $\xi \gg 1$, the asymptotic behavior of the pressure force becomes:

$$T_{rr} \quad = \quad \frac{1}{(t_c - t)^{1+1/n}} \frac{\alpha^2 A^2 \left(1 + 4\lambda^2 n^2 \right)}{2n^2} \xi^{-2(1+1/n)}, \tag{18}$$

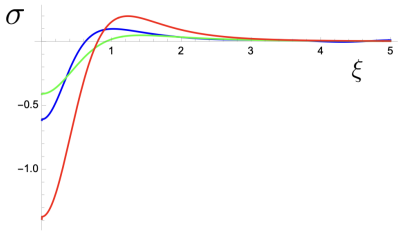

Figure 2: Plot of the self-similar the stress tensor $\sigma(\xi)$ as a function of the self-similar variable ξ. The plot includes the stresses computed in the following cases: $D = 1$, $n = 3$ (blue), $D = 2$, $n = 2$ (green), and $D = 3$, $n = 1$ (red).

for $\xi \gg 1$. We show the spatial variation of the singularity impulsive reaction (the self-similar function σ) for 1, 2, and 3 space dimensions on Figure 2. The most characteristic feature is that the singular solution always produces a singular pressure peak since in (17) $1+1/n > 0$. Other observables, as the dissipation rate, may not as we will see next.

3.3. Dissipative regularization of the singularity.

When the dissipation term $-i\nu\Delta^2\psi$ is added to the dynamics, leading to a viscous NLS equation:

$$i\frac{\partial\psi}{\partial t} = -\frac{\alpha}{2}\boldsymbol{\nabla}^2\psi - g|\psi|^{2n}\psi - i\nu\Delta^2\psi, \tag{19}$$

the singularity is suppressed, meaning that the inviscid finite-time singularity is regularized by the viscous term acting at short scales (and thus high amplitude). Indeed, one can deduce from the self-similar variable $\xi = r/(t_c - t)^{1/2}$, that the dissipation term diverges like $\nu(t_c - t)^{-2}\psi$ when approaching the singularity. It thus becomes dominant there, curing the finite-time singularity that is replaced by a finite amplitude peak. This can be seen by considering, using numerical simulations the time evolution with the viscous term $-i\nu\Delta^2\psi$ of an initial small density bump that would lead to a finite-time singularity for the NLS equation (2). In this case, as illustrated in figure (3) for the 2D case with $n = 2$ and $\nu = 10^{-4}$, we observe the formation in time of a peak that reaches a maximum value at some time.

As we follow in time the bump amplitude on figure 4 (a), which corresponds to the maximum of the square of the modulus wave function $\max|\psi|^2$, we notice that the formation of the first peak is followed by an oscillatory dynamics corresponding to successive density peaks localized also at the initial bump location. It should also be noticed that these peaks are well localized in time, the smaller the viscosity, the shorter, the more frequent and the higher are the peaks.

In fact, adding the viscous term to the NLS equation cancels the conservation laws of the dynamics and particularly the mass (5) and energy (8). Since the energy (8) has not a well defined sign, the quantity of interest for such simplified model is the mass (5) which is positive and dissipated by the viscous term, as

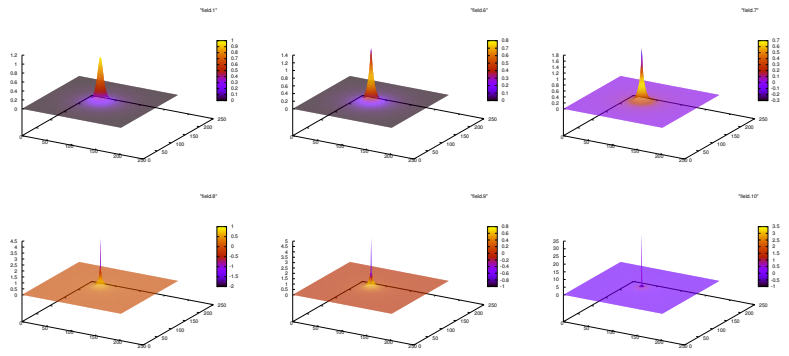

Figure 3: Snapshot of the density field $|\psi|^2$ at different times for a numerical simulation of the damped 2D NLS equation (19) with $n = 2$ starting with a small initial bump (top left figure). We observe the formation of a very thin peak localized at the center of the original bump, that reaches a maximum value up to 30 times the initial bump amplitude (bottom right). The viscosity is $\nu = 10^{-4}$ and the times of the snapshots correspond $t = 0.1$, 1.2, 1.4, 1.6, 1.8 and 2 from left to right and top to bottom.

proposed in our former study [9]. Indeed, the dissipation rate $\epsilon(\boldsymbol{x}, t)$, that is the loss of mass density per unit of time due to the dissipation term is directly deduced from the damped NLS equation (19), yielding for the variation of the total mass:

$$\frac{dN}{dt} = -2\nu \int |\Delta\psi|^2 d^D\boldsymbol{x} = -\int \epsilon(\boldsymbol{x}, t)\, d^D\boldsymbol{x},$$

where the dissipation rate as a function of space and time is defined through

$$\epsilon(\boldsymbol{x}, t) = 2\nu|\Delta\psi|^2. \tag{20}$$

From now on, it is useful to define the spatial averaged density and dissipation rate following

$$\bar{N}(t) = \frac{1}{L^D}\int_{L^D} |\psi|^2 d\boldsymbol{x}\,, \quad \text{and} \tag{21}$$

$$\bar{\epsilon}(t) = \frac{2\nu}{L^D}\int_{L^D} |\Delta\psi|^2 d\boldsymbol{x}\,. \tag{22}$$

In fact, throughout the paper, we will denote the spatial average of a quantity q by $\bar{q}$, and the temporal averages by $\langle q\rangle$, so that $\langle\bar{\epsilon}\rangle$ denotes the spatio-temporal average. Figure 4 (b) shows then the mean mass dissipation rate $\bar{\epsilon}(t)$ as a function of time for $\nu = 10^{-4}$ corresponding to the bump oscillations shown on figure 4 (a). It demonstrates that the $|\psi|^2$ peaks correspond exactly to peaks of the mass dissipation rate. More precisely, in the model, the dissipation (of mass) is concentrated in the violent events due to the singular dynamics of the inviscid dynamics. Remarkably however, we observe in this curve that these dissipation peaks increase with time as if the peaks are on top of an increasing

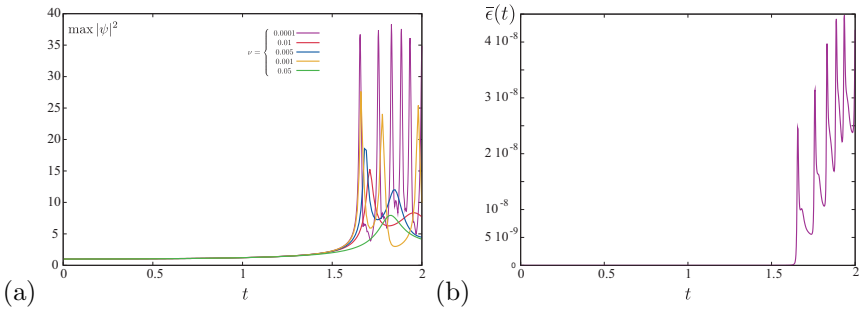

Figure 4: (a) The evolution of the maximum of the wave function modulus $\max|\psi|^2$ with time for a single damped singularity ruling the unforced but damped 2D NLS equation (19) with $n = 2$. The initial condition is a smooth bump for the different viscosities, $\nu = 10^{-4}$, 10^{-3}, $5 \cdot 10^{-3}$, 10^{-2} and $5 \cdot 10^{-2}$, the smaller the viscosity, the higher the peak amplitude. (b) The dissipation rate $\bar{\epsilon}(t)$ as a function of the time for the case $\nu = 10^{-4}$.

curve that we interpret as the dissipation rate coming from concentric waves generated by the density peaks (as it can be qualitatively observed on Figure 3.

In order to characterize these dissipation peaks, let us focus now on the dissipation rate that would induce a finite-time singularity using the inviscid single self-similar collapse (12), but estimating the dissipation rate of this solution at a non-zero viscosity ν, yielding:

$$\epsilon(t) = 2\nu(t_c - t)^{D/2-1/n-2} \int_0^\infty |\Delta_\xi \varphi|^2 \, \xi^{D-1} d\xi.$$

The total dissipation rate would therefore diverge in time in this framework as $t \to t_c$, following $\epsilon(t) \sim (t_c - t)^{-11/6}$ for $D = 1$ and $n = 3$ as studied in [9], and $\epsilon(t) \sim (t_c - t)^{-3/2}$ for $D = 2$ and $n = 2$ as studied here. The viscosity eventually regularizes this singular behavior consistent with the sharp peak of the mean dissipation observed in the numerics of figure 4 (b). Notice that in three space dimensions ($D = 3$) with $n = 1$, it is coincidently the same exponent, $\epsilon(t) = 2\nu(t_c - t)^{-3/2}$. We underline that for the NLS equation in higher dimensions, *e.g.* $D > 6$ and $n = 1$, the solutions of NLS (2) blow-up in finite-time, while the dissipation rate $\epsilon(t)$ does not.

Finally, we conclude noticing that in our numerics, we observe that the dissipation peak decreases with the viscosity, while the frequency peak increases so that the spatio-temporal averaged dissipation remains finite as $\nu \to 0$, as observed in 1D [9].

4. A turbulent behavior mediated by singularities

4.1. Forcing and dissipation: a simple turbulence framework

Adding a random forcing at large scale to the former dissipative model provides an idealized framework to investigate how a turbulent regime can emerge from a dynamics which contains finite-time singularities in the inviscid limit. We thus consider the equation (1) rewritten here:

$$i\frac{\partial\psi}{\partial t} = -\frac{\alpha}{2}\boldsymbol{\nabla}^2\psi - g|\psi|^{2n}\psi - i\nu\Delta^2\psi + f(\boldsymbol{x},t),$$

where the forcing term $f(\boldsymbol{x},t)$ is modeled in the Fourier space as a white noise with a Gaussian amplitude, namely:

$$\hat{f}_{k_0}(\boldsymbol{k},t) = a_0 w(t) e^{-\frac{k^2}{k_0^2}}.$$

Here a_0 is the forcing amplitude, while $w(t)$ is a homogenous complex random noise inside a sqare of radius 1 and centered at the origin in the complex plane.

The time variation of the total mass N reads now:

$$\frac{dN}{dt} = -\int \epsilon(\boldsymbol{x},t)\, d^D\boldsymbol{x} + i\int \left(\psi\bar{f}_{k_0} - \bar{\psi}f_{k_0}\right)\, d^D\boldsymbol{x}, \tag{23}$$

Therefore, in strong analogy with fluids, the dissipation density $-\epsilon(\boldsymbol{x},t)$ is strictly negative while the forcing can be positive or negative. As already said, we will focus only on $N(t)$ with its dissipation balance (23). We have shown that in the presence of forcing and dissipation the NLS equation (1) provides a genuine scenario for a singularity-mediated turbulence in 1D [9]. There, we have obtained that: i) the dissipation takes place near the singularities only, ii) such intense events are random in space and time, iii) the mean dissipation rate is almost constant as the viscosity varies, and iv) we observed an Obukhov-Kolmogorov spectrum with a power law dependence together with an intermittent behavior characterized by structure functions correlations. We now seek to investigate how such model generalizes in 2D.

By "turbulent" we mean a disordered or chaotic spatio-temporal behavior given by the solutions of the partial differential equations (like (1)) where mass (N) and energy (H) are injected at large scale by a forcing term $f_{k_0}(x,t)$, while the viscous term dissipates them at small scales. Such turbulent dynamics is illustrated on figure 5 for two different viscosity $\nu = 10^{-3}$ (left) and $\nu = 10^{-4}$, (right) and two different forcing amplitudes $a_0 = 0.2$ (top) and $a_0 = 0.5$ (bottom). We observe qualitatively that the number of peaks increases with the forcing amplitude, while their height increases as we lower the viscosity, particularly for the higher forcing.

The numerical simulations show the existence of a permanent turbulent regime that is illustrated on Fig. 6, where the mean mass $\bar{N}(t)$ and energy $\bar{H}(t)$ are plotted as functions of time for the lower forcing $a_0 = 0.2$. There we observe that both the total mass and energy reach rapidly a stationary statistical regime where forcing and dissipation balances and $\bar{N}(t)$ fluctuates around a

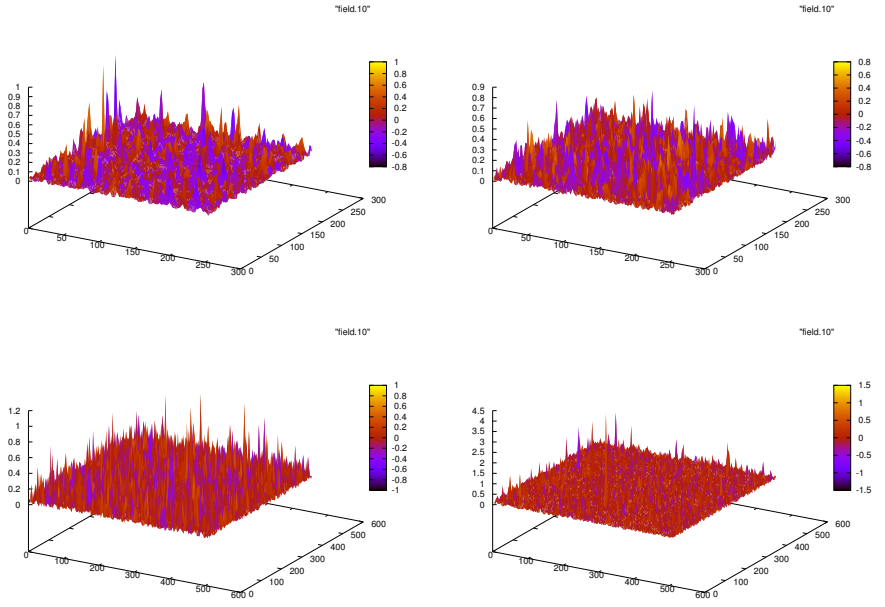

Figure 5: Density fields $|\psi(\boldsymbol{x},t)|^2$ solutions of the forced and viscous NLS equation (1) for $\nu = 10^{-3}$ (left) and $\nu = 10^{-4}$, (right) in the turbulent regime, for $D = 2$ and $n = 2$. The computational box size is 512×512 and the forcing is obtained using $k_0 = 0.5$ and $a_0 = 0.5$. We observed that the field is composed of many density peaks randomly distributed, the lower the viscosity, the higher the peaks.

mean value that is not depending strongly on the viscosity. Notice that in these cases the total energy displays negative values, a necessary condition for the genesis of a potential singularity (reminding the blow-up conditions, equation (11).

The mean (in space) dissipation rate, Fig. 7, exhibits a (statistically steady) randomly distributed sequence of peaks, in close correspondence with turbulent dissipation [14]. In our picture, these peaks correspond to the formation of singularities stopped by the viscosity.

4.2. The turbulent dissipation rate

As observed in Ref. [9] in one space dimension the total dissipation rate shows a sequence of intermittent appearance of peaks of dissipation which are reminiscent of the inviscid blow-up solution of the NLS equation (2). These peaks do not present any singularity because viscosity regularizes a potential singular behavior. Varying viscosity, but keeping all the other parameters constant, it is observed similar phenomenology than in 1 D [9]. As in one space dimension, in the numerics we observe that the strength of the dissipation peaks decreases with the viscosity, and the recurrence time for the appearance of peaks increases so that, the spatio-temporal averaged dissipation rate remains finite.

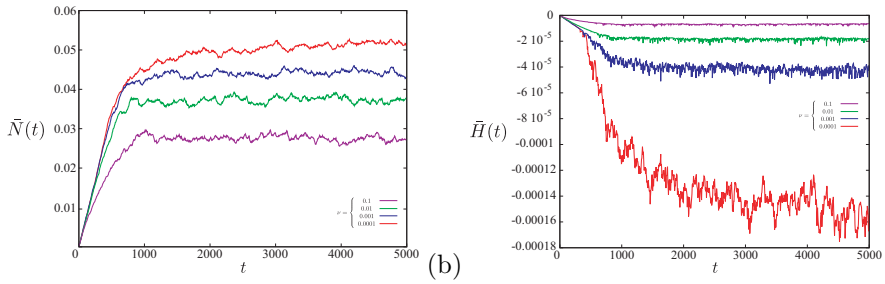

Figure 6: The mean density (21) and mean energy density versus time for various numerical simulation of the viscous forced NLS model (1). The is done numerics for $D = 2$ and $n = 2$, the forcing is $a_0 = 0.2$ and various dissipation as show in the plots.

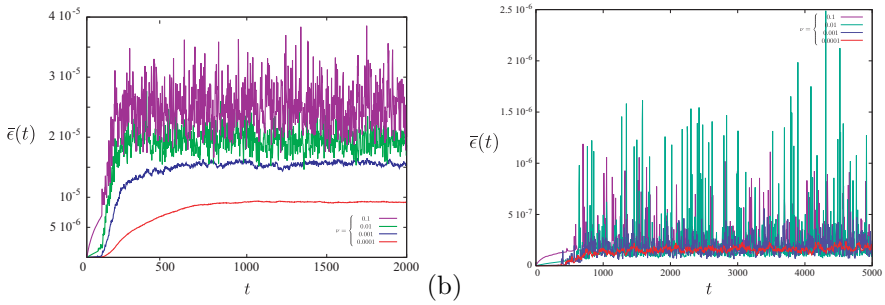

Figure 7: The mean dissipation rate $\bar{\epsilon}(t)$ defined by eq. (20) vs. time for various numerical simulation of the viscous forced NLS model (1) for an amplitude of the forcing (a) $a_0 = 0.2$ and (b) $a_0 = 0.5$ for $k_0 = 0.5$ for dissipation varying for $\nu = 10^{-1}$ to $\nu = 10^{-4}$ as shown in the plots. Remark that although the temporal average $\langle\bar{\epsilon}\rangle$ looks almost independent of viscosity for large forcing (panel b), for small forcing (panel a) there is an slight dependence of the time average $\langle\bar{\epsilon}\rangle$ as a function of ν.

The most remarkable feature is the observation of an "anomalous dissipation" effect. More precisely, the mean (in space and time) dissipation rate, $\langle\bar{\epsilon}\rangle$, is almost independent of viscosity as $\nu \to 0$ for a fixed forcing amplitude ($1/\nu$ is thus the analog of high Reynolds number here, see the dimensional analysis below) , as shown in Fig. 8 (a). This feature suggests that the injection purely selects the mean dissipation rate. The dissipative processes adapt to viscosity variations. This mechanism corresponds to the "anomalous dissipation" in the infinite Reynolds number limit, where mean dissipation converges to a constant value as the viscosity decreases [15].

Although $\langle\bar{\epsilon}\rangle$ is almost constant as a function of viscosity, as in one space dimensions, for intermediate forcing, the ratio between the dissipation peaks over the mean dissipation rate, $\epsilon_{\text{peak}}/\langle\bar{\epsilon}\rangle$ exhibits a critical behavior as viscosity varies (See Fig. 8 (b)). This plot shows the average of the dissipation peaks normalized by the mean dissipation rate $\langle\bar{\epsilon}\rangle$ vs $1/\nu$. As $\nu \to 0$, or $1/\nu \gg 1$ the dissipation peaks decrease. The maximum ratio arises for a viscosity of the order of $\nu = 10^{-3}$ in dimensionless units. This feature was also observed in one

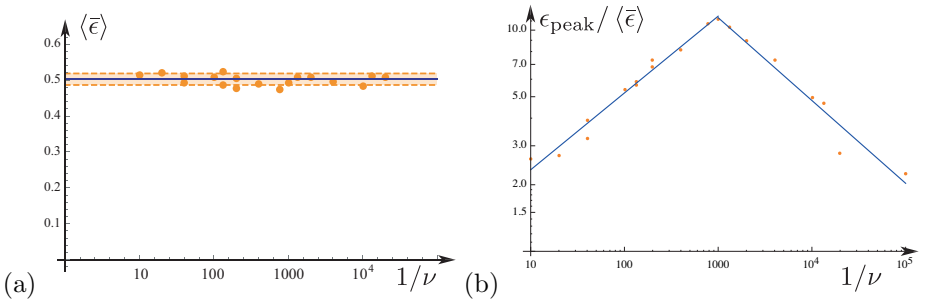

Figure 8: (a) The mean dissipation rate defined by eq. (20) vs. the inverse of viscosity $1/\nu$. The mean dissipation rate is $\langle\bar{\epsilon}\rangle = 0.5025 \pm 0.016$ and almost constant up to a 3%. (b) Mean peak dissipation created by the intermittent events, normalized by the mean dissipation rate, as a function of the inverse of viscosity. One observes that the peak events may be as large as 10 times the mean dissipation rate. The curves corresponds to the fits $\epsilon_{\rm peak}/\langle\bar{\epsilon}\rangle = 1.051\,\left(\frac{1}{\nu}\right)^{0.347}$ for $1/\nu < 1000$, and $\epsilon_{\rm peak}/\langle\bar{\epsilon}\rangle = 151\,\nu^{0.374}$ for $1/\nu > 1000$. The numerical simulations of the viscous forced NLS model (1) are done for $D = 2$ and $n = 2$. The system size is $L = 9.7$ units and a forcing $a_0 = 0.1$.

space dimensions [9], but, unfortunately, at this stage, a rational explanation of this striking effect is still missing.

As the forcing is changed this overall picture remains unchanged. The mean dissipation rate is almost independent of viscosity, except, perhaps, for small forcing (see $a_0 = 0.01$ in Figure 9 (a)) where one notices an apreciable non constant tendency for various measurements. Figure 9 (b) shows that the non-monotonic behavior of $\epsilon_{\rm peak}/\langle\bar{\epsilon}\rangle$, still exhibits a maximum around $\nu \approx 10^{-3}$.

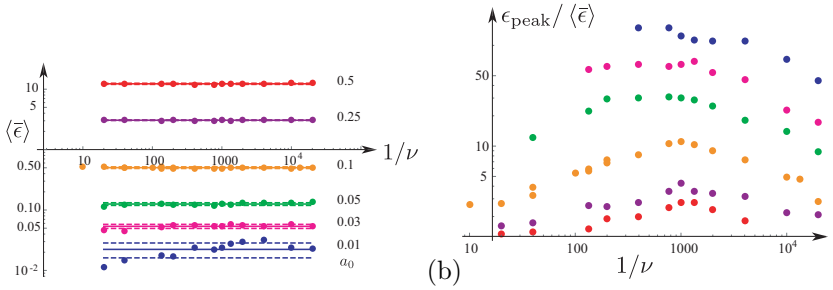

Figure 9: (a) The mean dissipation rate for various forcing, as function of the inverse of the dissipation coefficient ν. The plot shows that for almost all values of a_0 the mean dissipation rate is almost independent of viscosity. (b) Mean peak dissipation created by the intermittent events, normalized by the mean dissipation rate, as a function of the inverse of viscosity for various forcing. In both plot •: $a_0 = 0.5$, •: $a_0 = 0.1$, •: $a_0 = 0.01$, •: $a_0 = 0.25$, •: $a_0 = 0.05$, •: $a_0 = 0.03$.

We end this section, noticing two interesting features that discriminate the $1D$ from the $2D$ cases. In two space dimensions the mean dissipation rate in space and time are much larger than in one space dimensions, that is

$$\langle\bar{\epsilon}\rangle_{2D} \gg \langle\bar{\epsilon}\rangle_{1D}\,.$$

On the contrary, the peak-mean ratio is about a hundred times smaller than the same quantity in one space dimensions, that is

$$\epsilon_{peak}/\,\langle\bar{\epsilon}\rangle_{2D} \ll \epsilon_{peak}/\,\langle\bar{\epsilon}\rangle_{1D.}$$

Finally, in Fig. 10 we observe that the mean dissipation rate scales like the square of the forcing amplitude $\langle\bar{\epsilon}\rangle_{2D} \sim a_0^2$.

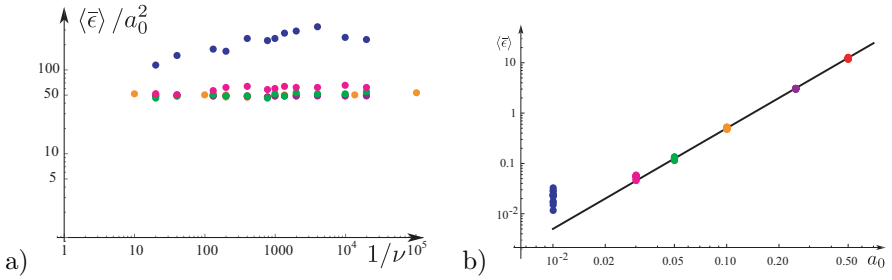

Figure 10: a) The mean dissipation rate of Fig. 9-a normalized by a_0^2 vs. the inverse of the dissipation coefficient ν. The plot shows that excepting for a small forcing $a_0 = 0.03$ all other points collapse in a single horizontal line. b) The mean dissipation rate $\langle\bar{\epsilon}\rangle$ vs. the forcing a_0 for various viscosities. The line represents the law $\langle\bar{\epsilon}\rangle \sim a_0^2$ as an eye-guide. Because the mean dissipation rate does not depend strongly on the viscosity all points overlap in a single point, excepting for the small forcing $a_0 = 0.03$ as in the left panel. The colors correspond to the same points of Figs. 9-a & b.

4.3. Dimensional analysis of the problem and discussion

In order to discuss our results, it is important to first perform a dimension analysis. We attribute to $|\psi|^2$ the dimensions of ϱ, that is $|\psi|^2 \sim \varrho$. Then, the parameters of the un-forced non-linear Schrödinger equation (1) scale as: $\alpha \sim \ell^2/\tau$, $g \sim 1/(\tau\varrho^n)$ and $\nu \sim \ell^4/\tau$, where ℓ and τ stand for the units of length and time respectively. Therefore we cannot define a dimensionless parameter from these equations parameters only playing a role similar to the Reynolds number in fluid mechaics. The additive complex forcing, $f(\boldsymbol{x}, t)$, in equation (1) must be included as a Wiener process, that is $|f^2|\,\Delta t$ has dimensions of ϱ, therefore the global turbulent problem (with forcing and dissipation) exhibits a single dimensionless number (first written in general, and then, using the specific values $D = n = 2$ of the current study, and recalling that the magnitude of the forcing is characterized by a_0):

$$\Pi = g|f|^{2n}\left(\frac{\nu}{\alpha^2}\right)^{n+1} = \frac{g a_0^4 \nu^3}{\alpha^6}. \tag{24}$$

This dimensionless number is however difficult to interpret since the forcing and the dissipation are on the same side of the fraction, in apparent contradiction with a Reynolds number that would involve a ratio of these two quantities.

However, as discussed above when plotting the dissipation rate, we can argue that Π represents the inverse of a Reynolds number of the problem for fixed forcing amplitude.

Contrarily to the Navier-Stokes equation, where there is no intrinsic length, in the current case the presence of the dispersion (the α term) and viscosity (ν term) introduces an intrinsic length, namely $\sqrt{\frac{\nu}{\alpha}}$. Therefore, considering the system size $L \sim \ell$ as an additional geometrical parameter, we can build another dimensionless number

$$\Pi_1 = \frac{\alpha L^2}{\nu}. \tag{25}$$

This parameter may be seen as the analogous of a Knudsen number, that is the ratio of the system size with a microscopic length. It is practically large in our simulations and should not play a crucial role *a priori* so that we will omit it in the further analysis.

Next, we perform the dimensional analysis on the mean observable quantities in the turbulent regime, namely $\left\langle \bar{N} \right\rangle \sim \varrho$ and $\langle \bar{\epsilon} \rangle \sim \varrho/t$.

For the dissipation rate we thus obtain:

$$\langle \bar{\epsilon} \rangle = a_0^2 \mathcal{F}_\epsilon(\Pi). \tag{26}$$

Our numerical simulations showing that the dissipation rate does not vary with the viscosity at first order suggest that we can consider there $\mathcal{F}_\epsilon(\Pi)$ as a constant, leading to the prediction $\langle \bar{\epsilon} \rangle \propto a_0^2$, as observed in the numerics (see Figure 10).

Similar analysis for the mean density gives: $\left\langle \bar{N} \right\rangle \sim \frac{\nu a_0^2}{\alpha^2} \mathcal{F}_N(\Pi)$. Here the numerical observation that $\left\langle \bar{N} \right\rangle$ varies only slightly with the viscosity leads to the prediction (seeking a power law behavior for the function $\mathcal{F}_N(\Pi) \propto \Pi^m$ such that the viscosity dependance disappears): $\left\langle \bar{N} \right\rangle \propto a_0^{2/3} g^{-1/3}$ that seems consistent with our results (N is increasing with the forcing less than the dissipation rate) although a detailed study should be performed in further studies.

Because of the variety of dimensionless quantities a pure Kolmogorov-like argument is not sufficient to provide a close formula for the spectrum. Indeed, following [9] we define the Fourier spectrum $S_k(t)$ by

$$S_k \equiv \left\langle |\hat{\psi}_{\boldsymbol{k}}|^2 \right\rangle \tag{27}$$

where the brackets $\langle \cdots \rangle$ stand here for the mean angular average and with the following definition of the Fourier transform:

$$\hat{\psi}_{\boldsymbol{k}}(t) = \frac{1}{L^{D/2}} \int \psi(\boldsymbol{x}, t) e^{-i\boldsymbol{k}\cdot\boldsymbol{x}} d\boldsymbol{x},$$

we obtain the relations:

$$\psi_k^2 \sim \ell^D \varrho \text{ and thus } a_0^2 \sim \ell^D \varrho/\tau^2.$$

Thus the Fourier spectrum, $S_k \sim |\hat{\psi}_k|^2 \sim \varrho \ell^D$. Since the spectrum depends *a priori* on the wave number k, the dimensional analysis suggests:

$$S_k = \frac{a_0^2}{\alpha}\left(\frac{\nu}{\alpha}\right)^{1+D/2}\mathcal{F}_S\left(\Pi, k\sqrt{\frac{\nu}{\alpha}}\right) = \frac{a_0^2\nu^2}{\alpha^3}\mathcal{F}_S\left(\Pi, k\sqrt{\frac{\nu}{\alpha}}\right).$$

In fact, the pertinent quantity for the spectrum should be the dissipation rate, so that we can easily transform this relation using eq. (26) into a Kolmogorov-like spectrum:

$$S_k = \frac{\epsilon\nu^2}{\alpha^3}\mathcal{G}_S\left(\Pi', k\sqrt{\frac{\nu}{\alpha}}\right),$$

where Π' is the equivalent dimensionless number based on ϵ instead of a_0:

$$\Pi' = g\epsilon^n\left(\frac{\nu}{\alpha^2}\right)^{n+1} = \frac{g\epsilon^2\nu^3}{\alpha^6}. \tag{28}$$

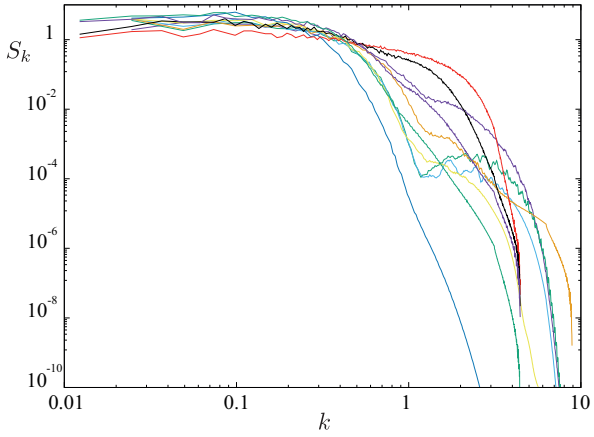

Figure 11: The Fourier spectrum (27) in the turbulent regime as a function of the wave number for two distinct forcing amplitudes $a_0 = 0.2$ and $a_0 = 0.5$ and viscosities ν varying form 10^{-4} to 0.1. The spectra seem to follow a scaling law $\langle S_k \rangle \sim$ const.

Figure 11 (a) shows the spectrum as function of the wave number k for two different forcing amplitudes ($a_0 = 0.2$ and 0.5) and different viscosities (from $\nu = 0.1$ to 10^{-4}), showing a plateau at large scale, that indicates, at first order at least, that the spectrum seems independent both on k and ν (the dependance on ϵ being difficult to determine since it does not vary too much for the different amplitude of forcing by contrast with the viscosity). The viscosity will then enter in the spectrum only through the spectral extension of the spectrum, defining a Kolmogorov scale of wavenumber k_ν above which the spectrum decreases rapidly. Using these numerical observations, the spectrum should follow by dimensional analysis:

$$S_k = A\frac{\alpha}{\epsilon^{1/3}g^{2/3}}, \tag{29}$$

where A is a numerical constant. Balancing the dissipation rate ϵ of this flat spectrum extending towards $k = k_\nu$, we obtain:

$$\epsilon \sim \int_0^{k_\nu} \nu k^5 S_k dk \sim \nu k_\nu^6 A\frac{\alpha}{\epsilon^{1/3}g^{2/3}},$$

leading to the definition of the Kolmogorov lengthscale:

$$\ell_\nu \sim \frac{1}{k_\nu} \sim \frac{(\nu\alpha)^{1/6}}{(g\epsilon^2)^{1/9}}.$$

However, if we rescale the different spectrum by the constant value $\frac{\alpha}{\epsilon^{1/3}g^{2/3}}$ and plot them as function of $k\ell_\nu$, we do not observe a clear collapse of the spectrum on a master curves, showing that a more detailed analysis on the turbulent spectrum should be performed (for instance considering a small dependance on the wave number, as observed in the 1D case [9]), that we postpone to furture studies.

5. Conclusions

A generic mechanism for the observed intermittency behavior of the dissipation rate in turbulence is proposed in the framework of the self-focusing nonlinear Schrödinger with dissipation and subjected to a random forcing. The toy-model display the remarkable property of anomalous dissipation, that is the dissipation rate does not depend on the dissipation mechanism as viscosity goes to zero. Additionally, the system displays a transition-like behavior for the measure of the peaks of dissipation normalized to the mean dissipation as viscosity diminishes. All behaviors are robust in one and two space dimensions.

Finally, we have investigated whether such turbulent dynamics that is strongly induced by the singular feature of the model gives rise to a continuum spectrum that could be viewed as due to a Kolmogorov-Richardson cascade where smaller structures are generated by the growth of instabilities in larger structures, as imagined by Kolmogorov. In 1D, we observed that despite the high intermittencies of the flow due to the intense peak of density, the mean spectrum did exhibit a power law dependance in $k^{-1/3}$ which is different than that of a peak, meaning that a genuine turbulent spectrum emerge from the random formation of the peaks. In two space dimensions, the dimensional analysis suggest a flat spectrum extending over a range selected by a Kolmogorov scale. However, the present numerical simulations do not clearly exhibit such behavior and a more detailed and specific analysis on the turbulent spectrum, as well as on the structure functions is postponed to further studies. Our results draw however some perspective while open questions remain: first of all, for the two space dimensions investigated, we observed a peak in the dissipation peak around a

given viscosity. Such a behavior is surprising and deserves a more precise analysis. The link, if any, between the singularities and the Kolmogorov-like spectra observed is unclear and an analysis going further than dimensional analysis is needed. Moreover, our model suggest that Kolmogorov spectrum can be compatible with finite time singularities, so that the transfert of a quantity (mass here, energy in other cases) from large to short scales might use short-cuts instead of cascades. In fact the two mechanisms are not in contradiction and could happen simultaneously, or the cascade could appear as a complex average process over a singularity, as highlighted for vortex collapses in fluids [16, 17]. It would thus be interesting to use recent time and space correlation functions that characterize irreversible processes to characterize the role of the singularities in the mass transfer here [18]. Finally, it would be also interesting to investigate similar models exhibiting finite time singularities, with a positive definite energy in particular, to observe how our result can generalize.

SR acknowledges support from FONDECYT (Chile) grant N° 1220369.

References

[1] J. Leray, Essai sur le mouvement d'un fluide visqueux emplissant l'espace, Acta Math. 63 (1934) 193–248.

[2] Y. Pomeau, Singularité dans l'évolution du fluide parfait, C. R. Acad. Sci. Paris 321 (1995) 407–411.

[3] Y. Pomeau, On the self-similar solution to the Euler equations for an incompressible fluid in three dimensions, Comptes Rendus Mécanique 346 (3) (2018) 184 – 197.

[4] T. M. Elgindi, Finite-time singularity formation for $C^{1,\alpha}$ solutions to the incompressible Euler equations on $\mathbb{R}^3$, Annals of Mathematics 194 (3) (2021) 647–727.

[5] S. Rica, Potential anisotropic finite-time singularity in the three-dimensional axisymmetric Euler equations, Phys. Rev. Fluids 7 (2022) 034401.

[6] A. Kolmogorov, Dokl. Akad. Nauk SSSR 30 (1941) 301 [English transl. in Proc. R. Soc. London **434**, 9 (1991) (In particular see the second footnote in page 10)].

[7] T. von Kármán, L. Howarth, On the statistical Theory of Isotropic Turbulence., Proc. R. Soc. Lond. 164 (1938) 192–216.

[8] U. Frisch, Turbulence: The legacy of A.N. Kolmogorov, Cambridge University Press, 1995.

[9] C. Josserand, Y. Pomeau, S. Rica, Finite-time localized singularities as a mechanism for turbulent dissipation, Phys. Rev. Fluids 5 (2020) 054607.

[10] V. Talanov, Self-focusing of wave beams in nonlinear media, JETP Lett. 2 (1965) 138–141.

[11] V. Zakharov, Zh. Eksper. Teoret. Fiz. 62 (1972) 1745 [English transl. in Sov. Phys. JETP **35**: 908 (1972)].

[12] B. LeMesurier, G. Papanicolaou, C. Sulem, P. Sulem, Focusing and multi-focusing solutions of the nonlinear Schrödinger equation, Physica D 31 (1988) 78–102.

[13] C. Budd, S. Chen, R. Russell, New self-similar solutions of the nonlinear Schrödinger equation with moving mesh methods, J. Comp. Phys. 152 (1999) 756–789.

[14] C. Meneveau, K. Sreenivasan, The multifractal spectrum of the dissipation field in turbulent flows, Nuclear Physics B - Proceedings Supplements 2 (1987) 49 – 76.

[15] K. R. Sreenivasan, On the scaling of the turbulence energy dissipation rate, The Physics of Fluids 27 (5) (1984) 1048–1051.

[16] T. Lundgren, Strained spiral vortex model for turbulent structures, Phys. Fluids 25 (1982) 2193–2203.

[17] Y. Cuypers, A. Maurel, P. Petitjeans, Vortex burst as a source of turbulence, Phys. Rev. Lett. 91 (2003) 194502.

[18] C. Josserand, M. L. Berre, T. Lehner, Y. Pomeau, Turbulence: does energy cascade exist?, J. Stat. Phys. 167 (2017) 596.